Python Supervised Co-simulation for A Day-long Harmonic Evaluation of EV Charging

Wang, L.; Qin, Z.; Beloqui Larumbe, L.; Bauer, P.

DOI
10.23919/CJEE.2021.000034

Publication date
2021

Document Version
Accepted author manuscript

Published in
Chinese Journal of Electrical Engineering

Citation (APA)
Wang, L., Qin, Z., Beloqui Larumbe, L., & Bauer, P. (2021). Python Supervised Co-simulation for A Day-long Harmonic Evaluation of EV Charging. *Chinese Journal of Electrical Engineering*, *7*(4), 15-24. https://doi.org/10.23919/CJEE.2021.000034

Python Supervised Co-simulation for A Day-long Harmonic Evaluation of EV Charging*

Lu Wang, *Zian Qin**, *Lucia Beloqui Larumbe and Pavol Bauer*
(Department of Electrical Sustainable Energy, Delft University of Technology, Delft 2628 CD, Netherlands)

Abstract: To accurately simulate electric vehicle DC fast chargers' (DCFCs') harmonic emission, a small time step, i.e., typically smaller than 10 μs, is required owing to switching dynamics. However, in practice, harmonics should be continuously assessed with a long duration, e.g., a day. A trade-off between accuracy and time efficiency thus exists. To address this issue, a multi-time scale modeling framework of fast-charging stations (FCSs) is proposed. In the presented framework, the DCFCs' input impedance and harmonic current emission in the ideal grid condition, that is, zero grid impedance and no background harmonic voltage, are obtained based on a converter switching model with a small timescale simulation. Since a DCFC's input impedance and harmonic current source are functions of the DCFC's load, the input impedance and harmonic emission at different loads are obtained. Thereafter, they are used in the fast-charging charging station modeling, where the DCFCs are simplified as Norton equivalent circuits. In the station level simulation, a large time step, i.e., one minute, is used because the DCFCs' operating power can be assumed as a constant over a minute. With this co-simulation, the FCSs' long-term power quality performance can be assessed time-efficiently, without losing much accuracy.

Keywords: Power quality, harmonic modeling, charging infrastructure for electric vehicles (EVs)

1 Introduction

For widespread electric vehicle (EV) adoption, fast-charging stations (FCSs) are being built along highways as crucial infrastructures that can alleviate EV customers' range anxiety for long-distance trips [1-2]. However, how the widespread installation of FCSs will affect the grid in terms of power quality remains unclear. A typical FCS is connected to the medium-voltage (MV) distribution grid and equipped with several high-power DC fast chargers (DCFCs) and a battery energy storage system (BESS) [2-3]. The DCFCs and BESS are connected to the distribution grid with power converters that comprise power electronics and power filters. Hence, an FCS is essentially a power-electronics-based system, which is the same as a wind farm or photovoltaic (PV) farm. Harmonic emission noncompliance and harmonic resonance, which have been reported in wind farms [4], PV farms [5-7], and other power-electronic-based systems [8], can be expected to happen in FCSs.

To study the impact of FCS on grid power quality, modeling and simulation of the FCS's harmonic performance are critical. However, making this simulation both accurate and time-efficient is quite challenging [9]. On one hand, a small time step (10 μs) is needed for accurate simulation of the switching frequency harmonics because a typical DCFC's switching frequency is normally above 20 kHz. On the other hand, according to the grid code, a one-day or even longer and continuous evaluation of harmonics is needed for the power quality assessment [10]. A simulation with a small time step for a day-long harmonic evaluation is not feasible due to either long simulation time or high computational cost.

To address this simulation challenge, a co-simulation is proposed, as illustrated in Fig. 1. Two simulation models operate simultaneously. One has a small time step (10 μs is chosen in this study) and sits in a

Manuscript received xxx; revised xxx; accepted xxx. Date of publication xxx; date of current version ****, 2020.
* Corresponding Author, Email: Z.Qin-2@tudelft.nl
* This project has received funding from the Electronic Components and Systems for European Leadership Joint Undertaking under grant agreement No. 876868. This Joint Undertaking receives support from the European Union's Horizon 2020 research and innovation programme and Germany, Slovakia, Netherlands, Spain, Italy.
Digital Object Identifier: 10.23919/CJEE.2021.000013

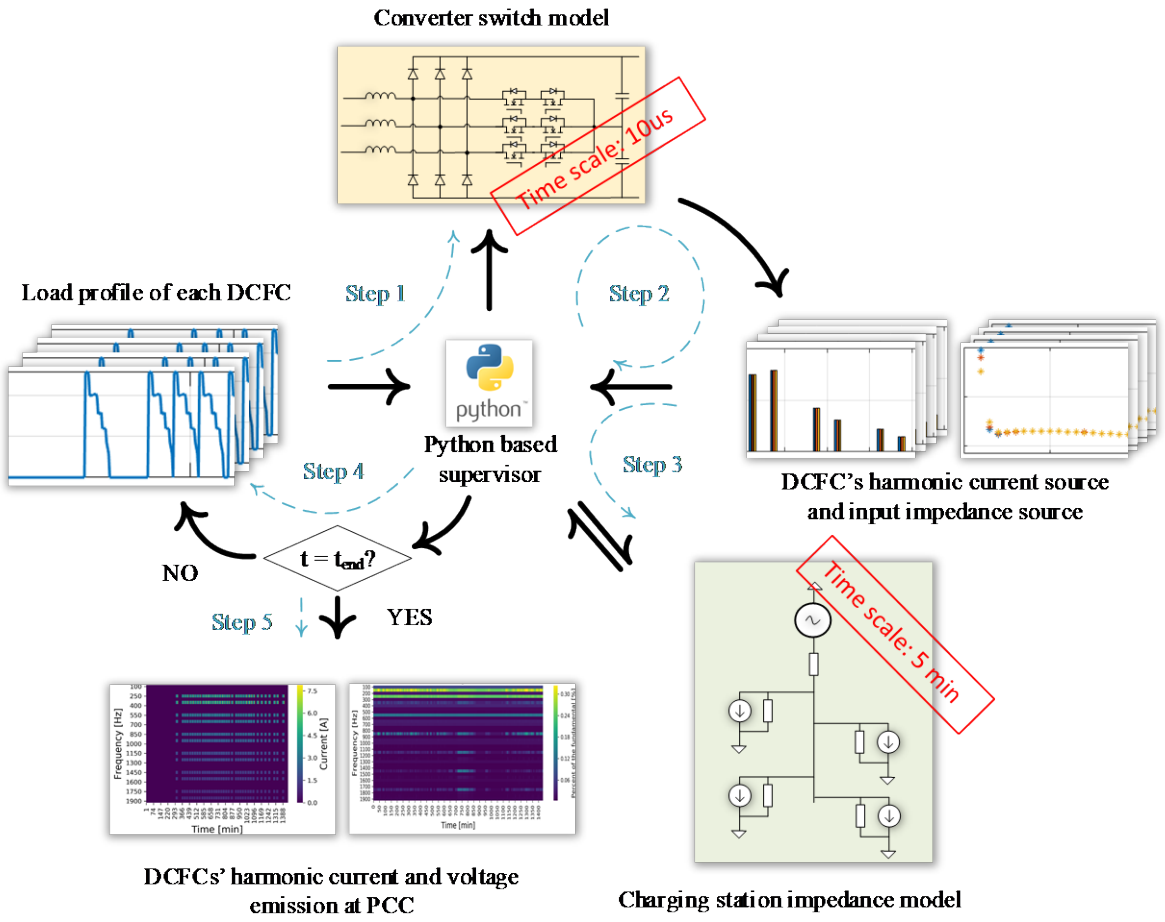

Fig. 1 Python supervised co-simulation for a day-long harmonic evaluation of EV charging

circuit simulation environment (PLECS in this study). The switching dynamics, current controller, and phase lock loop (PLL) of the DCFC are all modeled in detail. Based on this simulation model, the DCFC's input impedance and harmonic current source at certain operating power can be obtained. The other model has a large time step (one minute is chosen in this study) and sits in a system simulation environment (PowerFactory in this study). In the system model, all the DCFCs are simplified as Norton equivalent circuits, where the current sources and impedances are from the small step simulation model, as mentioned above. Consequently, the current sources and impedances are updated every minute, which is reasonable, because the charging power changes during one charging event but usually with a time step longer than one minute. For a certain charger, its Norton equivalent current source and input impedance only change when the charging power (or namely operation point) changes. Consequently, because the harmonic evaluation is based on the Norton equivalent model, the simulation is quick. Meanwhile, the Norton equivalent model is obtained from the switching model of the charger and is updated in real time. Thus, the impact of a time-variant charging profile is considered, and the evaluation accuracy is ensured. The co-simulation is implemented using a Python supervisor. More details are as follows.

Step 1: the operating power $P_x(t_i)$ of each DCFC is obtained, where $P_x(t_i)$ denotes the operating power of the DCFC x at time t_i.

Step 2: the DCFCs' input impedance $Z_x(t_i, f_h)$ and harmonic current source $H_x(t_i, f_h)$ at time t_i and harmonic frequencies f_h are estimated with the small timescale simulation. Here, the harmonic frequency denotes the frequency that is the integral multiple of the fundamental frequency in the range of 0–2 kHz.

Step 3: for the harmonic load flow simulation

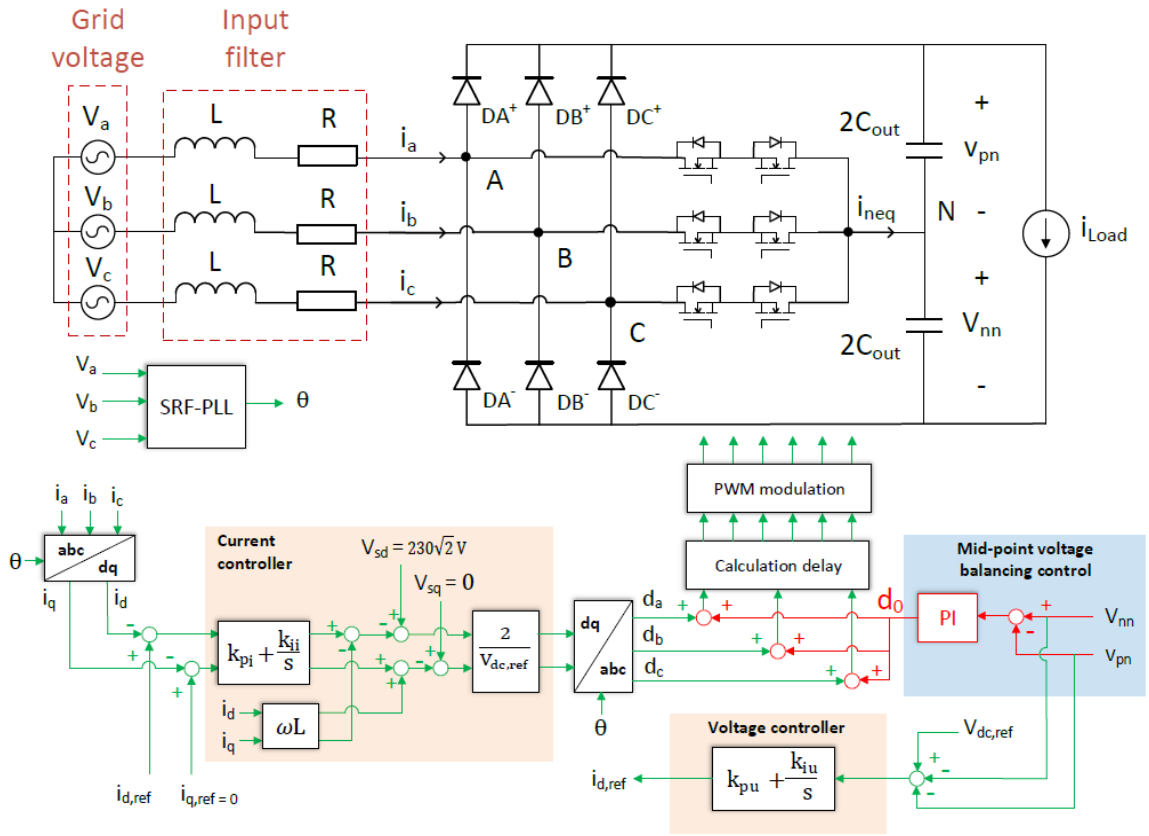

Fig. 2 Design of a typical 30-kW power module of the modeled DC fast charger

at t_i, each DCFC's input impedance and harmonic source in PowerFactory are updated to $Z_x(t_i, f_h)$ and $H_x(t_i, f_h)$, respectively, by the Python supervisor. The simulation result of PowerFactory at t_i is sent to the Python supervisor and recorded.

Step 4: the time step is updated to t_{i+1}, and the simulations are repeated. The iteration continues until all time steps in the load profile are finished. During the final step, the simulation results are visualized.

In the following sections, the modeling of DCFC and FCS is presented first. Afterward, the simulation results of the DCFC's input impedance and harmonic current source are presented. Thereafter, a one-day load profile simulation with a time resolution of one minute is performed to specify the DCFCs' operating points for that day. Later, based on the developed FCS model and load profile, the FCS's long-term harmonic performance can be simulated by updating the DCFCs' input impedance and harmonic current source per minute.

2 Modeling of the DC fast charger

2.1 Design of the DC fast charger

A typical DCFC comprises two power conversion stages, a front-end AC-to-DC stage and a DC-to-DC stage. The two stages are buffered with a DC link where high-capacitance capacitors are used for a stable DC voltage level. Hence, the DCFC's impact on power quality is mainly determined by the front-end converter.

As reported in Refs. [11-12], Vienna rectifier is a mainstream topology used for the DCFC's front-end converter because of its superior performance regarding reliability, power density, and efficiency. Thus, the Vienna rectifier is selected for the DCFC model. Additionally, modular design is typical for DCFCs, especially for those with high-power ratings, because of (1) the wide battery voltage range, (2) less stress on the power electronic components, (3) less design pressure on the cooling system, and (4) flexible compatibility with different EVs with different rated charging powers [2]. Based on the selection of Vienna rectifier and modular design concept, a 360-kW DCFC

comprising twelve 30-kW parallel power modules was designed. The DCFC's 30-kW power module design is illustrated in Fig. 2. In Tab. 1, the key parameters of the design are listed.

Tab. 1 Design parameters of the DCFC's power module

Parameters	Values
Line-to-neutral RMS voltage $V_{a\text{-}c}$/V	230
Inductor L/μH	250
Resistor R/mΩ	20
Capacitor C_{out}/μF	1 500
DC-link voltage V_{dc}/V	800
PLL bandwidth BW_{PLL}/Hz	100
Current loop bandwidth BW_{CL}/Hz	1 000
Voltage loop bandwidth BW_{VL}/Hz	400
Switching frequency f_s/kHz	20

As shown in Fig. 2, the feedback control of the Vienna rectifier consists of current control, voltage control, and mid-point voltage balancing control that ensure a small difference between V_{pn} and V_{nn}. The synchronous d-q frame PI controller [13] is used for current control. Additionally, the synchronous reference frame PLL (SRF-PLL) [13] is used to track the grid voltage phase. As digital control is used, a calculation delay of one switching cycle is considered in the model [14]. The pulse width modulation (PWM) [15-16] signal is obtained with the symmetrical modulation method, which induces a delay of half the switching cycle. Therefore, the whole delay caused by the control roughly equals 1.5 T_{sw}, where T_{sw} is one switching cycle period.

2.2 Input impedance modeling

Based on the DCFC's model shown in Fig. 2, the input impedance can be estimated analytically [13-14,17-19]. However, since the analytical model is based on an assumption that may lead to errors, a more accurate method is needed to obtain the input impedance via frequency sweep using either the switch model or real hardware.

As illustrated in Fig. 3, the input impedance can be measured by injecting a small voltage perturbation V_h at frequency f_h into the input 3-phase voltages. By measuring the harmonic component I_h at f_h of the

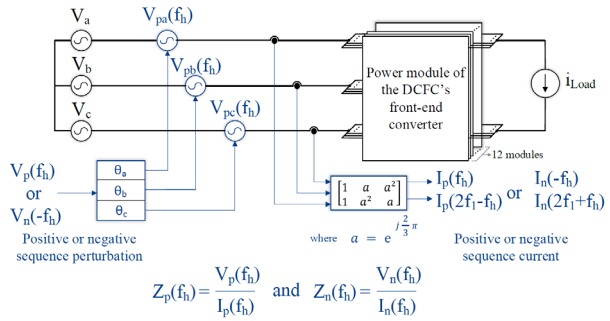

Fig. 3 Illustration of the frequency sweep for estimating the input impedance of the DC fast charger through numerical simulation

input current, the input impedance at f_h can be calculated. Notably, depending on the sequence of injected voltage perturbation, the measured input impedance is in the corresponding sequence domain, namely the positive or negative-sequence domain. Since the frequency coupling impedances are much higher compared to their counterparts at f_h [13], they are neglected for simplicity.

3 Modeling of the fast-charging station

3.1 Configuration of the fast-charging station

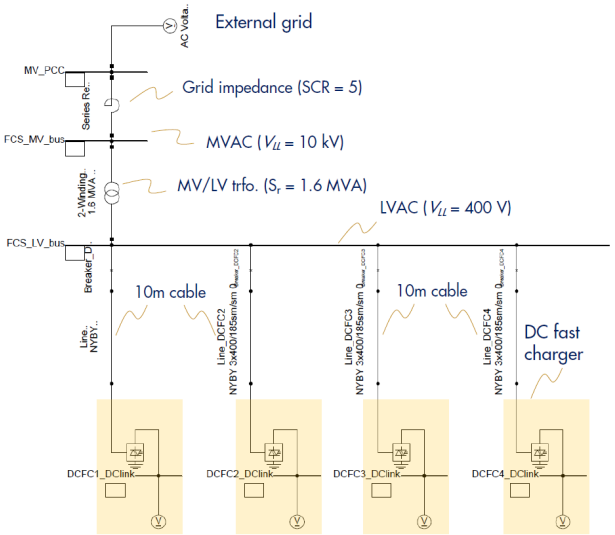

Fig. 4 Model of the fast-charging station with four 360-kW DCFCs in PowerFactory. Note that the chargers are simplified as their Norton equivalent circuit in the simulation

As illustrated in Fig. 4, an FCS with four 360-kW DCFCs was modeled. To fulfill the peak power demand with a certain safety factor, the service transformer has a capacity of 1.6 MVA. Additionally, since FCSs are usually constructed along highways, a

long distance between a substation and FCS is expected. Therefore, the FCS is connected to the external grid with a low short circuit ratio (SCR), e.g., SCR=5, which indicates a weak grid condition.

3.2 Modeling of the external grid

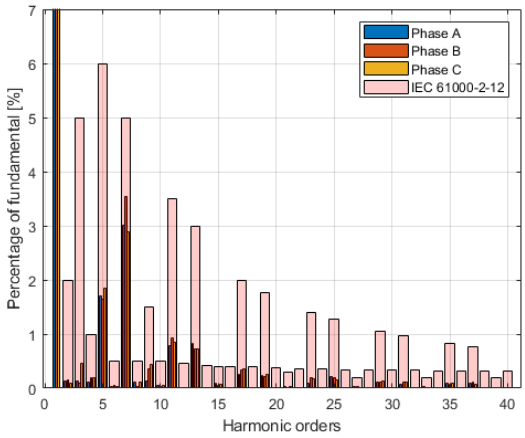

(a) Frequency spectrum of the background voltage

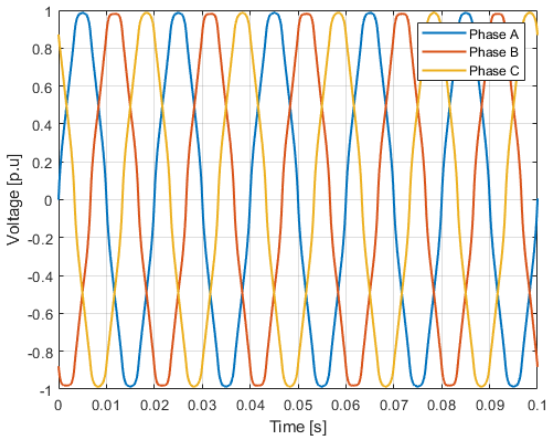

(b) Waveform of the background voltage

Fig. 5 Assumed harmonic voltages in the voltage of the grid to which the fast-charging station is connected

As reported in Ref. [20], a typical MV grid voltage has a total harmonic distortion (THD) of 2%, which is averaged yearly. However, in a worst-case scenario, a THD of 4% can be observed. Here, to evaluate the harmonic compliance of an FCS in certain severe conditions, the THD for the grid voltage is assumed to be 4%. The spectrum and time-domain waveform of the grid voltage are shown in Fig. 5. Notably, the harmonics of the assumed grid voltage are smaller than the recommended planning level in IEC 61000-2-12 [21].

3.3 Modeling of charging profile

Based on the arrival time, distribution of cars at a gasoline station in a day [22], and charging profile of Porsche Tycan, the load profile is generated by assuming that the state of charge of each car equals 10% before charging and reaches 80% after finishing charging. The time resolution of the generated load profile is reduced to one minute by assuming the arrival time of cars has an even hourly distribution. The resultant load profile is shown in Fig. 6.

At each simulation time step, the four DCFCs' input impedance and harmonic current source are updated according to their operating power. Thereafter, the harmonic load flow simulation in PowerFactory is conducted to evaluate the voltage harmonic at the low-voltage and MV bus bars.

Such a modeling method is also called quasi-dynamic modeling because the system dynamics within the simulation time step, i.e., one minute here, are ignored.

4 Simulation results and discussion

4.1 Input impedance of the DCFC

Based on the DCFC's model presented in Fig. 2 and the input impedance measurement method presented in Fig. 3, the DCFC's input impedance and harmonic current source at different operating powers (obtained from the load profile) are simulated. To show that the charger's impedance is influenced by the charging power, the simulation result shown in Fig. 7 compares the positive and negative-sequence impedances of the DCFC at 260, 120, and 58 kW, which are randomly selected operating powers in the load profile.

Fig. 7 shows that the operating power influences the positive sequence impedance only for frequencies smaller than 500 Hz. However, for the negative-sequence impedance, the operating power influences the entire range of 100 Hz to 2 kHz. Owing to the high switching frequency and subsequent low delay induced by digital control, the negative resistance region in the impedance reported in Ref. [13] is not observed in the presented frequency range.

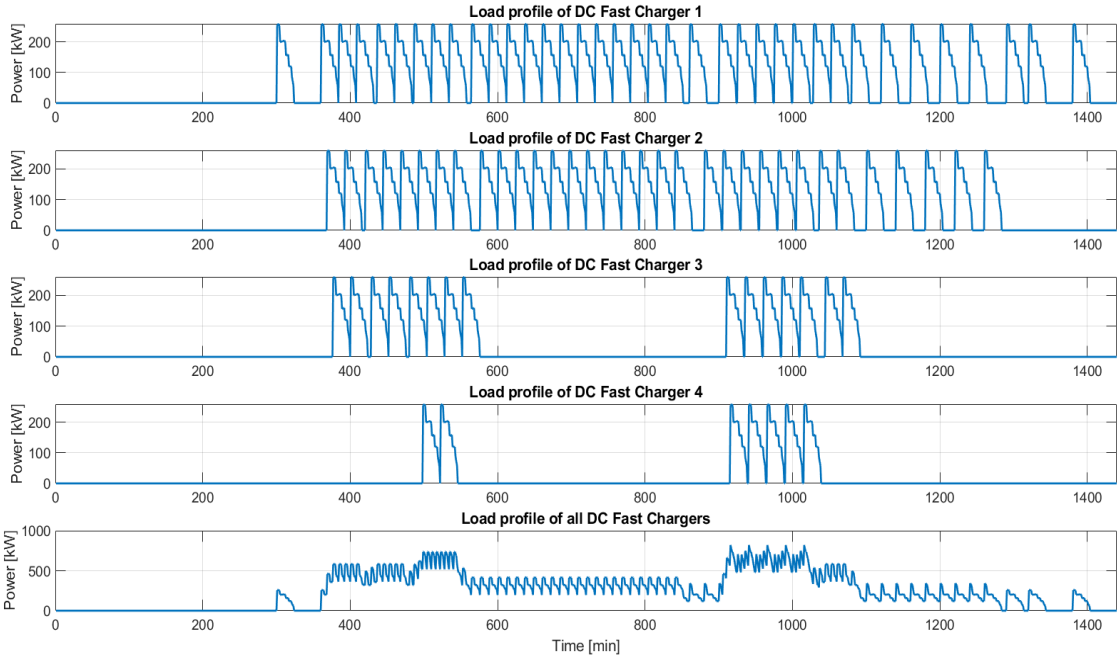

Fig. 6 Load profile of each charger and the fast-charging station

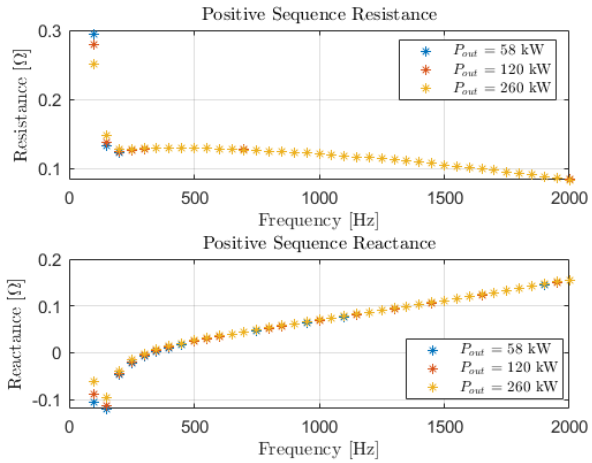

(a) Positive sequence impedance

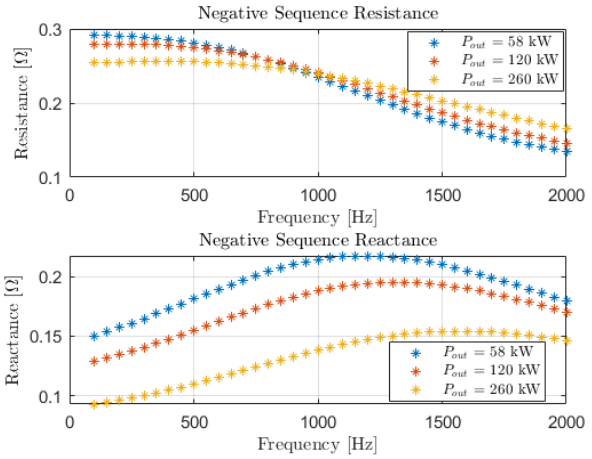

(b) Negative sequence impedance

Fig. 7 Input impedance of the DCFC at three charging power

Additionally, the DCFC's input impedance is low because of the use of modular design. Since the power modules of a DCFC are connected parallelly, the input impedance of the DCFC is reduced.

4.2 Harmonic current source of the DCFC

In Fig. 8, the input current waveform and its spectrum of the DCFC at 58, 120, and 260 kW are shown. To estimate the harmonic current source of the charger, the grid that the charger is connected to is ideal. The results show that the difference among the DCFC's harmonic current source at different operating points is significant. The harmonic current is higher when the DCFC operates at low power because the charger is designed to guarantee its harmonic compliance at nominal power. When the fundamental current is low with a comparable harmonic current component, the control performance worsens.

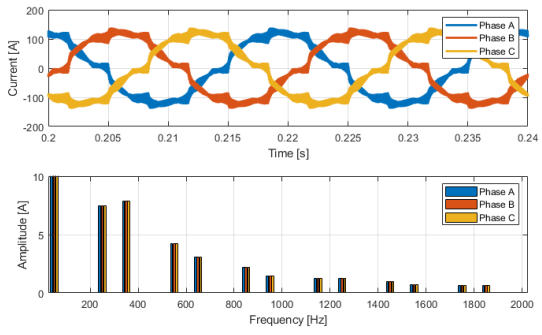

(a) 58 kW

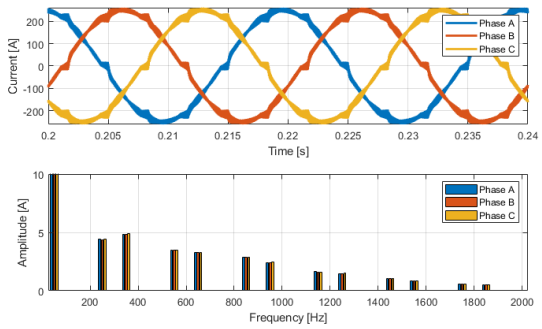

(b) 120 kW

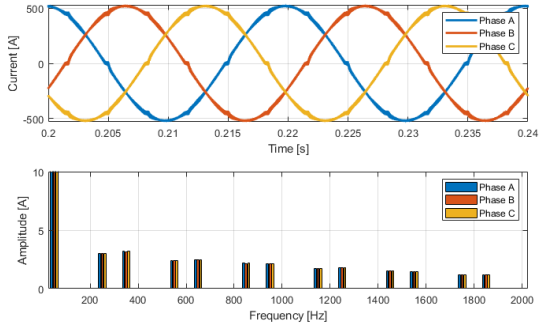

(c) 260 kW

Fig. 8 Variant harmonic current source of the DCFC at three charging power

4.3 Daily harmonic emission of the DCFCs

After the simulation iterations of all time steps, the harmonic current emission of the DCFCs in a day can be evaluated. The whole simulation takes roughly 2 h, which is much faster compared to the switching model. Moreover, given a load profile, the simulation can output the daily profile of the chargers' harmonic emission. Compared to the conventional approach, which only assesses the harmonic emission at several operating points of the charger, our approach is more comprehensive.

The simulation results of the harmonic current emission of each DCFC are presented in Fig. 9. As shown, the main harmonic emission of the charger is due to the 5^{th} and 7^{th} harmonic currents. That is because: (1) the 5^{th} and 7^{th} harmonic voltages are main in the background, and (2) the main primary harmonic emissions of the charger are due to 5^{th} and 7^{th} harmonic currents.

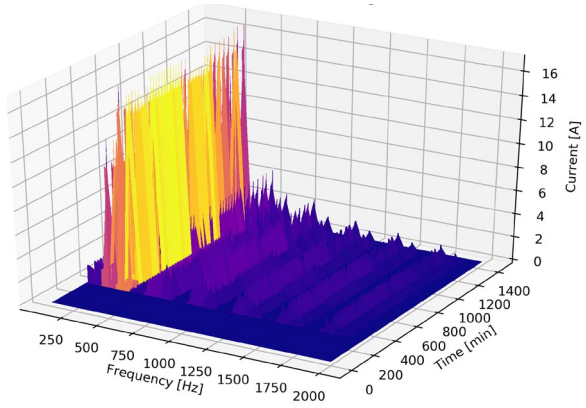

(a) Harmonic emission of charger 1

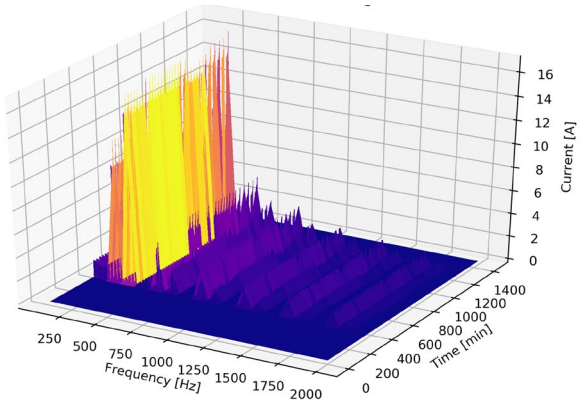

(b) Harmonic emission of charger 2

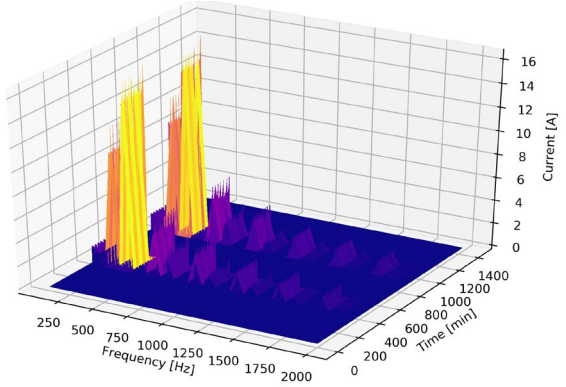

(c) Harmonic emission of charger 3

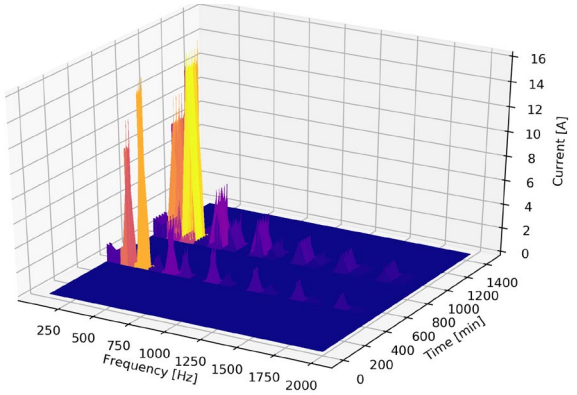

(d) Harmonic emission of charger 4

Fig. 9 Harmonic current emission of the four DCFCs in a day. Note that only one phase current is shown since the grid is assumed to be balanced

In Fig. 10, the main harmonics, namely 5th and 7th harmonics, and total demand distortion (TDD) of the four chargers in a day are illustrated and compared to the limits in the grid code IEEE 519. As shown, the TDD, 5th, and 7th harmonic currents are all below the limits described in IEEE 519. Fig. 10a shows that, when all the chargers are operating, e.g., t=1 000 min, the harmonic emission of the charger is slightly lower than that when only itself is operating, e.g., t=300 min. One possible reason is that the harmonic emission from the other chargers compensates for that induced by the distorted background voltage. To clarify the summation law of the harmonic emission from different chargers, more studies need to be conducted.

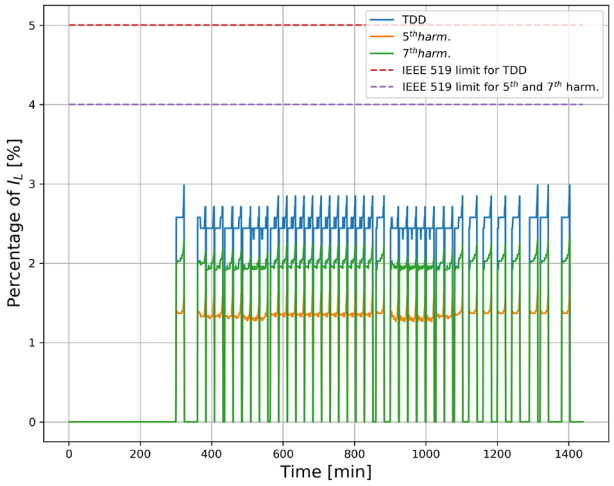

(a) Harmonic emission of charger 1

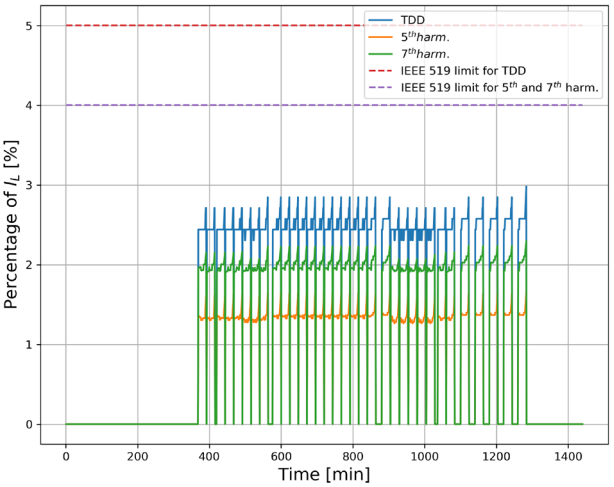

(b) Harmonic emission of charger 2

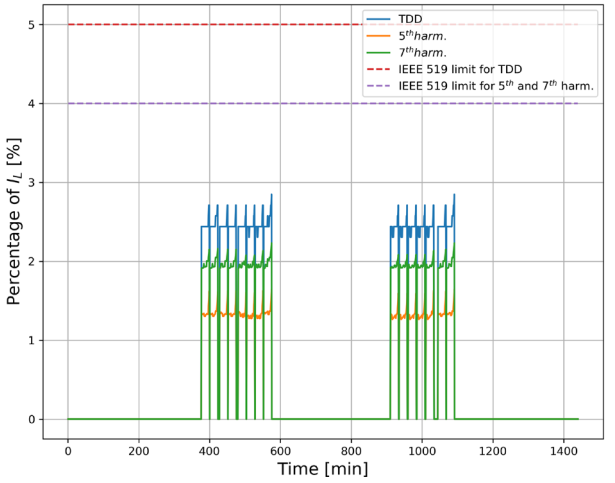

(c) Harmonic emission of charger 3

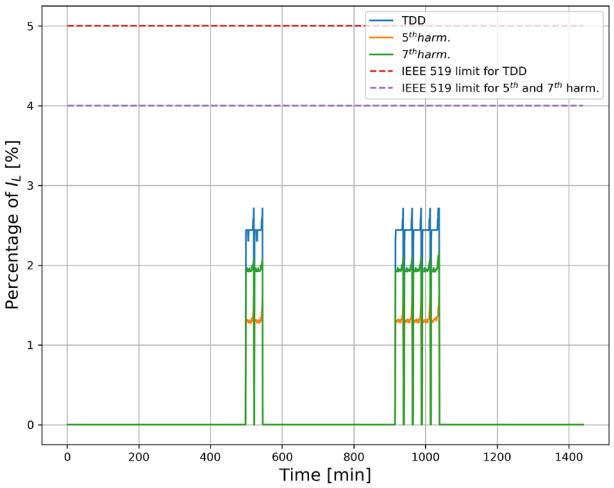

(d) Harmonic emission of charger 4

Fig. 10 Main harmonic current emission and the total demand distortion (TDD) of the four DCFCs in a day. Note that only one phase current is shown since the grid is assumed to be balanced. Note that I_L is the rated current

5 Conclusions

In this study, a Python supervised co-simulation for a day-long harmonic evaluation of EV charging is proposed and elaborated. The co-simulation consists of a switching model of the EV charger with a time step at the microsecond level, and a Norton equivalent model of the chargers with a time step at the minute level. The harmonic current source and impedance in the Norton equivalent model are updated in real time based on the information from the switching model. With such a co-simulation, a good balance between the accuracy and computational cost of the harmonic evaluation is achieved. For instance, a day-long

harmonic evaluation can be complete in two hours using a normal computer with our proposed co-simulation method. The simulation time can be further reduced if a more advanced computer is utilized. The effectiveness of the proposed co-simulation is verified by a case study, where the harmonic emission of a charging station is evaluated with a day-long charging profile.

References

[1] M Cheng, M Tong. Development status and trend of electric vehicles in China. *Chinese Journal of Electrical Engineering*, 2017, 3(2): 1-13.

[2] L Wang, Z Qin, T Slangen, et al. Grid impact of electric vehicle fast charging stations: Trends, standards, issues and mitigation measures-An overview. *IEEE Open Journal of Power Electronics*, 2021, 2: 56-74.

[3] S Srdic, S Lukic. Toward extreme fast charging: challenges and opportunities in directly connecting to medium-voltage line. *IEEE Electrification Magazine*, 2019, 7(1): 22-31.

[4] J H R Enslin, P J M Heskes. Harmonic interaction between a large number of distributed power inverters and the distribution network. *IEEE Transactions on Power Electronics*, 2004, 19(6): 1586-1593.

[5] L B Larumbe, Z Qin, P Bauer. Introduction to the analysis of harmonics and resonances in large offshore wind power plants. *in 2018 IEEE 18th International Power Electronics and Motion Control Conference (PEMC)*, Aug. 2018: 393-400.

[6] T Wang, H Nian, Z Q Zhu. Using inverter-based renewable generators to improve the grid power quality: A review. *Chinese Journal of Electrical Engineering*, 2018, 4(4): 16-25.

[7] J Lin, Y Li, S Hu, et al. Resonance mechanism analysis of large-scale photovoltaic power plant. *Chinese Journal of Electrical Engineering,* 2021, 7(1): 47-54.

[8] J Lei, Z Qin, W Li, et al. Stability region exploring of shunt active power filters based on output admittance modeling. *IEEE Transactions on Industrial Electronics*, 2021, 68(12): 11696-11706.

[9] L Wang, Z Qin, J Dong, et al. Design, modelling and evaluation of a GaN based motor drive for a solar car. *in IECON 2019-45th Annual Conference of the IEEE Industrial Electronics Society*, Oct. 2019, 1: 5120-5125.

[10] International Electrotechnical Commission. IEC 61000-4-7 Electro-magnetic compatibility (EMC) -Part 4-7: Testing and measurement techniques-General guide on harmonics and interharmonics measurements and instrumentation, for power supply systems and equipment connected thereto. Geneva: International Electrotechnical Commission, 2009.

[11] S Chon, M Bhardwaj, H Nene. Maximizing power for Level 3 EV charging stations[online]. Dallas: Texas Instrument, 2018[2021, Jul 21]. https://www.ti.com/lit/wp/sway014/sway014.pdf?ts=1632121602456&ref_url=https%253A%252F%252Fwww.ti.com%252Fsolution%252Fev-charging-station-power-module

[12] P Chatterjee, M Hermwille. Tackling the Challenges of Electric Vehicles Fast Chargings[Online]. Neubiberg: Infineon Technologies, 2020[2021, Jun 15]. https://www.infineon.com/dgdl/Infineon-Tackling_the_Challenges_of_Electric_Vehicles_Fast_Chargings-Article-v01_00-EN.pdf?fileId=5546d4626eab8fbf016f0c5d34f442fc

[13] M Cespedes, J Sun. Impedance modeling and analysis of grid-connected voltage-source converters. *IEEE Transactions on Power Electronics*, 2014, 29(3): 1254-1261.

[14] X Wang, L Harnefors, F Blaabjerg. Unified impedance model of grid-connected voltage-source converters. *IEEE Transactions on Power Electronics*, 2018, 33(2): 1775-1787.

[15] J Xu, J Han, Y Wang, et al. A novel scalar PWM method to reduce leakage current in three-phase two-level transformerless grid-connected VSIs. *IEEE Transactions on Industrial Electronics*, 2020, 67(5): 3788-3797.

[16] J Xu, J Han, Y Wang, et al. High-frequency SiC three-phase VSIs with common-mode voltage reduction and improved performance using novel tri-state PWM method. *IEEE Transactions on Power Electronics*, 2019, 34(2): 1809-1822.

[17] L B Larumbe, Z Qin, P Bauer. On the importance of tracking the negative-sequence phase-angle in three-phase inverters with double synchronous reference frame current control. *in 2020 IEEE 29th International Symposium on Industrial Electronics (ISIE)*, Jun. 2020: 1284-1289.

[18] L B Larumbe, Z Qin, P Bauer. Output impedance modelling and sensitivity study of grid-feeding inverters with dual current control. *in IECON 2019-45th Annual Conference of the IEEE Industrial Electronics Society*, Oct. 2019, 1: 4007-4012.

[19] B Wen, D Boroyevich, R Burgos, et al. Analysis of D-Q small-signal impedance of grid-tied inverters. *IEEE Transactions on Power Electronics*, 2016, 31(1): 675-687.

[20] L Derksen. Spanningswkaliteit in Nederland 2014[Online].

Den Haag: Movares Nederland B.V., 2015(2016, Sept 6)[2021, May 16]. https://www.vemw.nl/~/media/VEMW/Downloads/Public/Elektriciteit/Spanningswkaliteit%20in%20Nederland%202014.ashx

[21] International Electrotechnical Commission. IEC 61000-2-12 Electromagnetic compatibility (EMC) - Part 2-12: Environment-Compatibility levels for low-frequency conducted disturbances and signalling in public medium-voltage power supply systems. Geneva: International Electrotechnical Commission, 2003.

[22] K Yunus, H Z De La Parra, M Reza. Distribution grid impact of plug-in electric vehicles charging at fast charging stations using stochastic charging model. *in Proceedings of the 2011 14th European Conference on Power Electronics and Applications*, Aug. 2011: 1-11.

Lu Wang (S'20) was born in Sichuan, China. He received the B.Sc. degree in Electrical Engineering from Beijing Institute of Technology, Beijing, China, in 2015, M.Sc. degree (cum laude) in Electrical Power Engineering from Delft University of Technology, Delft, The Netherlands, in 2018, where he is currently pursuing the Ph.D. degree with the DC Systems, Energy Conversion and Storage group.

From 2019 to 2020, He was a hardware engineer at Prodrive Technologies B.V., Son, The Netherlands. His research interests include power quality and EV charging infrastructures.

Zian Qin (M'15-SM'19) received the B.Eng. degree in Automation from Beihang University, Beijing, China, in 2009, M.Eng. degree in Control Science and Engineering from Beijing Institute of Technology, Beijing, China, in 2012, and Ph.D. degree from Aalborg University, Aalborg, Denmark, in 2015.

He is currently an Assistant Professor in Delft University of Technology, Delft, Netherlands. In 2014, he was a Visiting Scientist at Aachen University, Aachen, Germany. From 2015 to 2017, he was a Postdoctoral Research Fellow in Aalborg University. His research interests include wide bandgap devices, power electronics based grid and Power2X.

He is an associate editor of IEEE Trans Industrial Electronics, guest associate editor of IEEE Journal of Emerging and Selected Topics and IEEE Trans Energy Conversion. He is a "distinguished reviewer" for the year 2020 of IEEE Transactions of Industrial Electronics. He served as the technical program chair of IEEE-ISIE 2020, technical program co-chair of IEEE-COMPEL 2020, industrial session co-chair of ECCE-Asia 2020.

Lucia Beloqui Larumbe (S'18) was born in Pamplona, Spain, in 1993. She received the B.Sc. and M.Sc. degrees in Electrical Engineering, in 2015 and 2017, respectively, from the Public University of Navarre, Pamplona, Spain. She did her Master's thesis at the Delft University of Technology, Delft, The Netherlands, on the topic of advanced control for microgrids. In 2017, she joined the DC systems, Energy conversion and Storage group (DCE\&S) at the Delft University of Technology, where she is currently pursuing a Ph.D. degree. Her research interests include control of power electronics, power quality, and renewable energies.

Pavol Bauer (SM'07) is currently a full Professor with the Department of Electrical Sustainable Energy of Delft University of Technology and head of DC Systems, Energy Conversion and Storage group.

He received Masters in Electrical Engineering at the Technical University of Kosice (a85), Ph.D. from Delft University of Technology (a95) and title prof. from the president of Czech Republic at the Brno University of Technology (2008) and Delft University of Technology (2016). He published over 72 journal and almost 300 conference papers in my field (with H factor Google scholar 43, Web of science 20), he is an author or co-author of 8 books, holds 4 international patents and organized several tutorials at the international conferences. He has worked on many projects for industry concerning wind and wave energy, power electronic applications for power systems such as Smarttrafo; HVDC systems, projects for smart cities such as PV charging of electric vehicles, PV and storage integration, contactless charging; and he participated in several Leonardo da Vinci and H2020 EU projects as project partner (ELINA, INETELE, E-Pragmatic) and coordinator (PEMCWebLab.com-Edipe, SustEner, Eranet DCMICRO).